**Atmospheric
Chemistry
and Physics
Discussions**

Technical Note: New trends in column-integrated atmospheric water vapor – Method to harmonize and match long-term records from the FTIR network to radiosonde characteristics

R. Sussmann[1], T. Borsdorff[1], M. Rettinger[1], C. Camy-Peyret[2], P. Demoulin[3], P. Duchatelet[3], E. Mahieu[3], and C. Servais[3]

[1]Research Center Karlsruhe, IMK-IFU, Garmisch-Partenkirchen, Germany
[2]Laboratoire de Physique Moléculaire pour l'Atmosphère et l'Astrophysique (LPMAA), CNRS/UPMC/IPSL, Paris, France
[3]Institute of Astrophysics and Geophysics, University of Liège, Liège, Belgium

---

Title Page

Abstract	Introduction
Conclusions	References
Tables	Figures

| ◄◄ | ►► |
| ◄ | ► |

| Back | Close |

Full Screen / Esc

Printer-friendly Version

Interactive Discussion

Abstract

We present a method for harmonized retrieval of integrated water vapor (IWV) trends from existing, long-term, measurement records at the ground-based mid-infrared solar FTIR spectrometry stations of the Network for the Detection of Atmospheric Composi-
5 tion Change (NDACC). Correlation of IWV from FTIR with radiosondes shows an ideal slope of 1.00(3). This optimum matching is achieved via tuning one FTIR retrieval parameter, i.e., the strength of a Tikhonov regularization constraining the derivative (with respect to height) of retrieved water profiles given in per cent difference relative to an a priori profile. All other FTIR-sonde correlation parameters (intercept $=0.02(12)$ mm,
10 bias $=0.02(5)$ mm, standard deviation of coincident IWV differences ($stdv$)$=0.27$ mm, $R=0.99$) are comparable to or better than results for all other ground-based IWV sounding techniques given in the literature. An FTIR-FTIR side-by-side intercomparison reveals a strong exponential increase in $stdv$ as a function of increasing temporal mismatch starting at $\Delta t \sim 1$ min. This is due to atmospheric water vapor variability. Based
15 on this result we derive an upper limit for the precision of the FTIR IWV retrieval for the smallest $\Delta t (=3.75$ min) still giving a statistically sufficient sample (32 coincidences), i.e., precision (IWV$_{FTIR}$)<0.05 mm (or 2.2% of the mean IWV). The bias of the IWV retrievals from the two different FTIR instruments is nearly negligible (0.02(1) mm). The optimized FTIR IWV retrieval is set up in the standard NDACC algorithm SFIT 2 with-
20 out changes to the code. A concept for harmonized transfer of the retrieval between different stations deals with all relevant control parameters; it includes correction for differing spectral point spacings (via regularization strength), and final quality selection of the retrievals (excluding the highest residuals (measurement minus model), 5% of the total).
25 The method is demonstrated via IWV trend analysis from the FTIR records at the Zugspitze (47.4° N, 11.0° E, 2964 m a.s.l.) and Jungfraujoch (46.5° N, 8.0° E, 3580 m a.s.l.) NDACC stations. Trend analysis comprises a linear fit after subtracting an intra-annual model (3 Fourier components) and constructing an uncertainty interval (95%

confidence) via bootstrap resampling. For the Zugspitze a significant trend of 0.79 (0.65, 0.92) mm/decade is found for the time interval (1996–2008). There is a significantly increased trend of 1.41 (1.14, 1.69) mm/decade in the second part of the time series (2003–2008) compared to 0.63 (0.20, 1.06) mm/decade in the first part

5 (1996–2002). For the Jungfraujoch no significant trend is found in any of the periods (1988–2008), (1996–2008), (1996–2002), or (2003–2008). The results imply either an altitude dependency with a significantly higher trend below 3.58 km than above, and/or strong, regional variations of IWV trends on the scale of ~250 km. This is in line with a widespread, complex, IWV trend picture over Eurasia during the last decades. Our

10 paper provides a basis for future exploitation of more than a dozen existing, multi-decadal FTIR measurement records around the globe for joint IWV trend studies within NDACC that complement existing trend data sets which are based primarily on radiosondes.

1 Introduction

15 Integrated water vapor (IWV) is a key climate variable. In the lower troposphere, condensation of water vapor into precipitation provides latent heat which dominates the structure of tropospheric diabatic warming. Water vapor is also the most important gaseous source of infrared opacity in the atmosphere. It accounts for about 60% of the natural greenhouse effect for clear skies and provides the largest positive feedback

20 in model projections of climate change. Accurate measurements of IWV are therefore one of the most important input parameters for climate models, i.e. measured IWV trends are important because they may be indicators of anthropogenic climate change. However, evidence for long-term changes in IWV is limited by the availability and quality of measurements (Trenberth et al., 2007).

25 Data for the last three or four decades of the twentieth century indicate an increase in water vapor in the lower troposphere over parts of the Northern Hemisphere. Up to now, trend studies of IWV have mainly been based on radiosondes (e.g., Ross and El-

liott, 2001). However, homogeneity of the radiosonde records was affected by changes in instrumentation and reduction of sounding activities. E.g., the major changes in US radiosonde types at the end of 1995 led to spurious changes dependent on time of observation, elevation, location, and season. In terms of moisture, there was a spuri-
5   ous drying, but mainly in the upper troposphere. In the lower troposphere, the relative humidity decreased from 5% to 8% with the switch from VIZ to Vaisala sondes (Elliott et al., 2002). A series of changes were made in the Vaisala sensor types used at operational stations in the first few years after 2000 and significant inter-sensor biases have been identified (e.g., Miloshevich et al., 2006).
10   Beginning in 1987, satellite-based data from microwave instruments provided improved observations of IWV. For example, data from the Special Sensor Microwave/Imager (SSM/I) have been exploited for investigation of IWV trends (Wentz and Schabel, 2000). However, key aspects of any, satellite-based dataset used to study decadal or longer timescales are changes in instrumentation and algorithms.
15   For instance, the number of SSM/I instruments used in the NASA Water Vapor Project (Randel et al., 1996; Vonder Haar et al., 2003) dataset has ranged from one (1988–1992) to three (Vonder Haar et al., 2005). So it is not surprising that a number of publications have noted that statistically significant, long-term trends in climate variables are difficult to derive from satellite data because of problems with satellite intercalibra-
20   tion and sensor drift (Hurrel and Trenberth, 1997, 1998; Christy et al., 1998; Wenz and Schabel, 1998; Trenberth et al., 2007). First satellite based IWV trend studies via ERS-2/GOME and ENVISAT/SCIAMACHY data were reported only recently (Wagner et al., 2006; Mieruch et al., 2008).

  Clearly, it is important to re-examine internally consistent, existing and ongoing long-
25   term records from other independent sounding techniques that contain information on IWV. One valuable source of data has turned out to be ground-based microwave radiometry (e.g., Morland et al., 2006; Fiorucci et al., 2008). Such measurements are being carried out to some extent within the NDACC[1] network, which is dedicated to

---

[1]*N*etwork for the *D*etection of *A*tmospheric *C*omposition *C*hange, http://www.ndacc.org

R. Sussmann et al.

long-term, ground-based, atmospheric sounding observations at many stations around the globe.

In addition, long-term observations using ground-based, mid-infrared solar FTIR spectrometry are organized within NDACC by the IRWG[2]. At its annual meetings during the last 15 years or so, a best-practice for FTIR measurements has been set up. This guarantees both high-level inter-station comparability and long-term stability of the measurements. Recently, IRWG activities have been extended to support harmonization of retrieval approaches.

This paper is a contribution to this effort. Although FTIR has been used for retrieval of numerous other species, it is clear that solar infrared spectra contain a considerable amount of information on water vapor as well. However, up to now there have been few attempts to retrieve water vapor from FTIR. The lack of sufficiently accurate spectroscopic data in the spectral domains of interest has been a major hindrance. However, it has been shown by Sussmann and Camy-Peyret (2002) that using the new, mid-infrared, water vapor spectroscopy from Toth and coworkers included in HITRAN 2000 (Rothmann et al., 2003) that information on water in the 11.7–11.9 µm region from solar spectra can be retrieved without the severe, spectral residuals due to line parameter errors left by HITRAN 1996 (see Figs. 9–14 in Sussmann and Camy-Peyret, 2002). Subsequently, Schneider et al. (2006) showed the first water vapor profile retrieval from ground-based FTIR spectrometry. This retrieval was optimized to obtain profile information, especially in the upper troposphere.

Retrievals of IWV from NDACC-type FTIR measurements still need to be systematically optimized before best-possible IWV data for trend studies can be obtained. There are more than a dozen FTIR stations around the globe with time series data covering more than one decade so that it is possible to create a substantial, complementary IWV set of trends.

The purpose of this paper is to develop an FTIR retrieval optimized for IWV which can be used to complement the radiosonde records. Section 2 presents a new method

---

[2]*Infrared Working Group*, http://www.acd.ucar.edu/irwg/

for optimizing IWV retrievals from FTIR measurements so that they match radiosonde characteristics. It includes a concept for station-to-station harmonization of the retrieval as well as error characterization. Section 3 demonstrates the method via retrieval of harmonized IWV series from the long-term FTIR records obtained at the Zugspitze (1996–2008) and Jungfraujoch (1988–2008) NDACC stations. It presents the analysis of IWV trends and their significance and discusses the trend results. In Sect. 4, we summarize our work and its potential in global trend studies.

2 Method

2.1 Retrieval strategy

An IWV retrieval from ground-based, mid-infrared solar FTIR spectrometry has been set up to i) yield an accuracy and precision comparable to the best among the other ground-based IWV sounding techniques, ii) match IWV retrieval response with standard radiosonde characteristics (i.e., correlation slope equals 1.0), and iii) implement it in the retrieval algorithm SFIT 2 (Pougatchev et al., 1995), which is the standard within the NDACC IRWG, without performing any changes to the code. The retrieval is thereby easily transferable to all ground-based, FTIR measurement stations of the NDACC network.

The classical approach to retrieve column integrated quantities from ground-based FTIR spectrometry has used least squares spectral fitting with iterative scaling of an (inflexible) *VMR*[3] a priori profile via one (unconstrained) altitude-constant factor (e.g., Rinsland et al., 1984). Because of the free scaling, this approach has the advantage that it does not damp true column variability in the retrieval. However, it frequently leads to significant spectral residuals (measurement minus model). This is because of i) likely discrepancies of the shape of the true profile relative to the a priori profile and

---

[3] *V*olume *M*ixing *R*atio

ii) possible spectral line shape errors in the forward calculation and/or the measurement. Both effects can introduce significant biases to the retrieved columns.

A strategy to reduce this problem is to derive total columns from (flexible) profile retrievals which help to better integrate the area of the measured absorption line shape and thereby obtain a more accurate estimate of the total column integral (even allowing, to some extent, for retrieval of unphysical profile shapes to compensate for line shape errors). Up to now, most profile retrievals from solar FTIR spectrometry have been regularized via diagonal a priori covariance matrices. This type of profile retrieval has, however, the tendency to damp variability in the retrieved total columns as a result of profile smoothing at the cost of any deviation between the retrieved profile and the a priori profile. In particular, this damping is a critical issue in the case of water vapor because of its high natural variability, which covers more than one order of magnitude in IWV.

Therefore, we have developed an IWV retrieval that combines the advantages of both a profile scaling and a profiling approach while avoiding their disadvantages at the same time. In other words, we construct a regularization matrix that allows for some (constrained) flexibility in profile shape (degree of flexibility to be tuned) and also guarantees that pure profile-scaling type variations remain unconstrained. This is achieved by imposing a Tikhonov first order smoothing constraint to retrieve per cent changes of the water vapor *VMR* profile relative to the a priori profile. Part of the strategy to optimally constrain the total water vapor column is to search for a set of spectral microwindows which contain information on the water vapor profile throughout the troposphere.

2.2 Retrieval set up

Figure 1 shows the spectral microwindows (i.e., the measurement vector *y*) which have been selected from a spectroscopic point of view with two different targets in mind. First, these windows completely avoid interference errors (Sussmann and Borsdorff, 2007) resulting from absorbing, telluric species other than water vapor. There is only

one small and narrow solar OH line seen in Fig. 1a. Since it is difficult to perfectly simulate such lines, we eliminated any resulting perturbations of the retrieval by deweighting the $\mathbf{S}_\varepsilon$ matrix accordingly (i.e., setting the signal-to-noise ratio to zero in the spectral vicinity of this line). Second, the microwindows are selected to yield sensitivity for water vapor variations throughout the whole troposphere to constrain the total column in the best possible way for a wide range of IWV levels. This is achieved by a using well-balanced mixture of strong and weak absorption lines.

The forward model $\mathbf{F}$ maps the water vapor profiles to be retrieved from state space $\boldsymbol{x}$ into measurement space $\boldsymbol{y}$. Figure 1 shows the final forward calculation of a retrieval performed using the HITRAN 2000 line parameters compilation (Rothman et al., 2003). The residuals in Fig. 1 show a perfect fit down to the noise level without any systematic residuals due to spectroscopic errors.

The retrieval is the (ill-posed) inverse mapping from $\boldsymbol{y}$ to $\boldsymbol{x}$ which is formulated as a least squares problem. Due to the non-linearity of $\mathbf{F}$, a Newtonian iteration is applied and a regularization term $\mathbf{R} \in \Re^{\cdot n \times n}$ is used that allows one to constrain the solution and thereby avoid oscillating profiles

$$
\begin{aligned}
\boldsymbol{x}_{i+1} = \boldsymbol{x}_i &+ \left(\mathbf{K}_{\boldsymbol{x},i}^T \mathbf{S}_\varepsilon^{-1} \mathbf{K}_{\boldsymbol{x},i} + \mathbf{R} \right)^{-1} \\
&\times \left\{ \mathbf{K}_{\boldsymbol{x},i}^T \mathbf{S}_\varepsilon^{-1} \left[\boldsymbol{y} - \mathbf{F}(\boldsymbol{x}_i) \right] - \mathbf{R}(\boldsymbol{x}_i - \boldsymbol{x}_a) \right\}
\end{aligned}
\tag{1}
$$

where the subscript i denotes the iteration index and $\boldsymbol{x}_a$ is the a priori profile. Here $\mathbf{K}_x = \partial \mathbf{F} / \partial \boldsymbol{x}$ are the Jacobians and $\mathbf{S}_\varepsilon$ is the measurement covariance (assumed to be diagonal with a signal-to-rms-noise ratio of 100 in our formulation). Using Tikhonov regularization (Tikhonov, 1963), $\mathbf{R}$ is setup by the relation

$$
\mathbf{R} = \alpha \mathbf{L}^T \mathbf{L} ,
\tag{2}
$$

where α is the strength of the constraint operator $\mathbf{L}$. We use the discrete first derivative

Trends in integrated water vapor from ground-based FTIR

R. Sussmann et al.

Title Page

Abstract	Introduction
Conclusions	References
Tables	Figures

◄◄	►►
◄	►
Back	Close

Full Screen / Esc

Printer-friendly Version

Interactive Discussion

operator $\mathbf{L}=\mathbf{L}_1$

$$\mathbf{L}_1 = \begin{pmatrix} -1 & 1 & 0 & \dots & 0 \\ 0 & -1 & 1 & \ddots & \vdots \\ \vdots & \ddots & \ddots & \ddots & 0 \\ 0 & \dots & 0 & -1 & 1 \end{pmatrix} \in \mathfrak{R}^{n \times (n-1)}, \tag{3}$$

which constrains x in a way such that a constant profile is favored for the difference $x - x_a$. The prior x_a is given in Fig. 2. It was constructed using data from a 3-month radiosonde campaign at the Zugspitze (see Sect. 2.3 for details). We use the mean profile scaled by 0.25 because otherwise retrievals for the driest days are not able to calculate a reasonable first iteration (because of saturated lines with no distinct line center position in a high IWV initial forward calculation).

The state vector x is set up on a 66-layer scheme with an exponential increase of layer width (0.162 km width for first layer above the Zugspitze site at 2964 m a.s.l. up to 5.292 km width for the last layer ending at 100 km a.s.l.). The state vector x is implemented in units of (dimensionless) scaling factors for the 66 layers relative to the a priori VMR profile (standard setting in SFIT 2). Therefore, the limiting case $\alpha \to \infty$ represents free scaling of the a priori *VMR* profile with one altitude-constant factor (i.e., an infinitely strong constraint to the profile shape and a zero constraint to the absolute value of the column). The limiting case $\alpha \to 0$ describes a retrieval without any regularization (which will suffer from oscillating profiles). The tuning of α to achieve an optimum IWV retrieval is described in the next section.

2.3 Matching FTIR to radiosonde characteristics

Section 2.2 left open the question of how to find an optimum setting for α. Figure 3a shows the correlation of IWV retrievals from Zugspitze FTIR measurements to coincident radiosondes for varied settings of α. Clearly, there is an impact of α on the quality of the correlation. Evidently, there is an impact on the slope of the linear fit to

the scatter plot. Figure 3b shows all correlation parameters derived from the scatter plots of Fig. 3a (and from a few more scatter plots which are not shown) as a function of α. It can be seen that an optimum correlation (i.e., slope $=1.0$) can be achieved for $\alpha_{opt}=183$, corresponding to a *dofs*[4] of 1.84. Figure 3c shows the underlying scat-

5 ter plot for this optimum setting with $R=0.99$, slope $=1.00$ and a negligible bias and intercept of 0.015 mm[5]. This means that it is possible to obtain a high-quality match between the FTIR retrieval and the radiosonde response, i.e., the measurements of the sonde and the FTIR no longer differ by a scaling factor after the matching.

Data for the 25 FTIR-sonde coincidences in Fig. 3 have been obtained during the

10 (19 Aug 2002–17 Nov 2002) AIRS validation campaign (Sussmann and Camy-Peyret, 2002, 2003) with FTIR measurements at the Zugspitze (47.4° N, 11.0° E, 2964 m a.s.l) and 180 radiosondes launched at Garmisch (47.5° N, 11.1° E, 734 m a.s.l.).

The 25 IWV data from Zugspitze FTIR (y-axis in Fig. 3a, c) were obtained by averaging the IWV typically retrieved from 3–4 individual spectra (each obtained from

15 15–20 min integration) recorded within ±1 hour around a $\sim 12{:}00$ UT fixed time (i.e., the time of AIRS overpass t_{op}).

The 25 IWV data from the Garmisch radiosondes (x-axis in Fig. 3a, c) were each obtained from integration of one "Tobin-sonde" VMR profile above the Zugspitze altitude. This profile was derived from a pair of soundings according to the "best-estimate of the

20 state of the atmosphere" principle (Tobin et al., 2006). I.e., a first sonde was launched 1 h before t_{op} and a second sonde 5 min before t_{op}. The best estimated humidity profile for the overpass time $VMR_{Tobin}(z, t_{op})$ was then constructed via inter-/extrapolation of the two soundings according to the relation

$$VMR_{Tobin}(z, t_{op}) = VMR_{sonde}(z, t_0) + (\mathrm{d}VMR(z)/\mathrm{d}t)(t_{op} - t_0), \qquad (4)$$

25 where for t_0 one uses the time of either of the two sondes at a level z as a starting point. See Fig. 3 in Sussmann and Camy-Peyret (2002) for an example.

---

[4] *d*egrees *o*f *f*reedom of *s*ignal, i.e., the spur of the averaging kernel matrix
[5] A water vapor column of 1 mm corresponds to $3.345 \cdot 10^{21}$ molecules/cm^2.

Trends in integrated water vapor from ground-based FTIR

R. Sussmann et al.

Title Page

Abstract | Introduction

Conclusions | References

Tables | Figures

|◄ | ►|

◄ | ►

Back | Close

Full Screen / Esc

Printer-friendly Version

Interactive Discussion

For this purpose two sonde receivers were used operating on two different frequencies in parallel (Vaisala Digicora III, Marwin 21, SPS220G sounding processor). Vaisala RS80-30G radio sondes were used (A-Humicap sensor). Several studies have been carried out to assess water vapor measurement accuracy of the RS80-A sonde and develop corrections for different classes of errors (Wang et al., 2002; Miloshevich et al., 2001, 2004, 2006; Leiterer et al., 2005; Suortti et al., 2008). Since we are interested in IWV, we quantified the known effect of the temperature-dependent dry bias (mainly at low temperatures) by applying the correction suggested by Leiterer et al. (2005); to visualize this see Fig. 1 (left center image) in Suortti et al. (2008). The effect of the correction on IWV is only of the order of 1 permille. We did not perform corrections for a possible overall bias from chemical contamination (e.g., term $\Delta_1 U$ in Leiterer et al., 2005), because i) no statistical correction data are available for our RS80-A production batch, ii) our later trend analysis is not impacted by the possible existence of FTIR biases, and iii) there is no significant overall bias of our optimized FTIR retrieval versus the sondes (Fig. 3c).

2.4 Precision and bias

Two FTIR instruments are operated side-by-side at the Jungfraujoch, one Bruker IFS 120 HR and one home-made instrument (see Sect. 3.1 for information on instruments and site). We transferred the optimized IWV retrieval developed and tested for the Zugspitze FTIR to the two Jungfraujoch instruments (see Sect. 2.6 for the transfer procedure). We have further taken advantage of the quasi-simultaneous measurements available from the two Jungfraujoch time series (essentially in the 1995–2001 time span) to derive precision and bias of the IWV retrieval. See Table 2 for the result.

The given numbers were derived as follows. We applied different temporal coincidence criteria Δt to the individual column retrievals of the two time series and created a scatter plot for each coincidence ensemble. From these scatter plots we obtained the standard deviation *stdv* of the differences of coincident FTIR pairs as a function of Δt, see Fig. 4 and first 3 rows of Table 1: starting at $\Delta t = 3.75$ min, a widening of Δt leads

to an monotonous increase of *stdv*. I.e., atmospheric variability dominates *stdv* even at the smallest time scale of minutes. Unfortunately one cannot use Δt=0 because there is a tradeoff between reducing Δt and the number of remaining coincidences. In our case, we stopped at Δt=3.75 min which still gave 32 coincidences. So in general,

5 the strictest temporal coincidence criterion which gives a sufficient statistical sample of coincidences would ideally be used to derive an estimate of IWV measurement precision from side-by side intercomparisons. Even in so doing, the estimate will always be an upper limit. For Δt=3.75 min, we obtain *stdv*=0.07 mm (3.1% of mean IWV) for the pairwise differences. Under the simplifying assumption of identical precision

10 for both FTIR systems, we calculate for the precision *prec* of one FTIR instrument: *prec*<*stdv*/sqrt(2) = 0.05 mm (or *prec*<2.2% of mean IWV).

A nearly negligible bias of 0.02(1) mm is found between the two Jungfraujoch FTIR instruments (for Δt=3.75 min). Note in Table 1, that the bias is not significantly altered when Δt is increased to 120 min.

15 **2.5   Comparison to other techniques**

Table 1 shows examples of comparisons of the different ground-based remote sounding techniques with radiosondes. First of all we discuss the comparison of the Zugspitze FTIR with Tobin sondes (4th row): The perfect slope of 1.00(3) is the result of our matching procedure where the intercept of 0.02(12) as well as the bias of 0.02(5) are

20 negligibly small. The *stdv* of the coincident differences is 0.27 mm (or 7.9%), which is much higher than the *stdv*=0.07 mm found in the FTIR-FTIR side-by-side intercomparison for Δt=3.75 min (1st row in Table 1). Clearly, the *stdv* of 0.27 mm is dominated by atmospheric variability within the coincidence interval Δt=120 min and the 8 km horizontal distance Δx between the FTIR and the sonde launching site. This interpretation

25 is in line with the observation that nearly the same *stdv*, i.e., 8.0%, is found in the FTIR-FTIR side-by-side intercomparison for Δt=120 min (3rd row in Table 1). In other words, no information on the precision of a ground-based sounder can be derived from a sonde intercomparison with a coincidence criterion of the order of 1–2 h, if the vertical

sounder has good precision as is the case for the FTIR.

As an example for a ground-based microwave instrument, we show the sonde-correlation data for TROWARA (taken from Morland et al., 2006) in the 5th row of Table 1. The slope is 0.88, the intercept 1.36 mm, and the bias 0.36 mm. The *stdv* of 2.02 mm is relatively high. This is a result of the large distance between TROWARA and the launching site of the sondes (Δx=40 km), i.e., the observed *stdv*=2.02 mm is not an appropriate measure of the (certainly significantly better) precision of TROWARA.

Morland et al. (2006) report correlating GPS and sun photometer (PFR) data with sondes (6th and 7th row of Table 1). The PFR shows a smaller bias (0.08 mm) than the GPS (0.53 mm). For both intercomparisons a relatively high *stdv* on the order of 1 mm is found, which is again certainly a result of the large Δx=80 km.

The FTIR-sonde correlation data shown in the 8th row of Table 1 have been taken from Palm et al. (2008). The slope is 0.85(1) and the intercept 0.66(9) mm. Comparing these numbers to the FTIR-sonde slope of 1.00(3) and intercept of 0.02(12) mm from our work (4th row), one has to keep in mind that the Palm et al. (2008) results originate from an FTIR retrieval which is different than the one described in our work.

The intercomparison data of BASIL (Raman lidar) and GBMS (microwave) with sondes (9th sand 10th row of Table 1) were taken from Fiorucci et al. (2008). Both instruments show slopes very close to 1, very small intercepts and biases below 0.1 mm. The *stdv* is also very small which is the result of the very strict, temporal coincidence criteria (Δt=20 min) and the fact that the sondes were launched right next to the ground-based vertical sounder (Δx=0).

2.6 Station-to-station harmonization

A crucial point of our approach is that it is implemented in the community-retrieval algorithm SFIT 2 (Pougatchev et al., 1995) without performing any changes to the code. The retrieval setup described in Sects. 2.2 and 2.3 can therefore be applied to all ground-based FTIR groups of the NDACC network which will allow harmonized network-trend studies on IWV. A first example for this is given in Sect. 3 for the case of

the Zugspitze and Jungfraujoch NDACC stations.

The algorithm harmonization is achieved via exchange of only a few control files, i.e., "binput" (containing among other fitting parameters the definition of microwindows shown in Fig. 1), "refmod" (containing the a priori profile given in Fig. 2; it should be applicable to all stations because there is no strong gradient around the tropopause), and the "cfgl-files" (containing the spectroscopic line list). Care has to be taken to use the same rule for setting up the exponential retrieval layer grid as described in Sect. 2.2 at all stations ("bnd-file"). This is important because the strength and altitude dependency of the effective regularization scheme depends on the details of the vertical grid.

In order to find a harmonized optimum α value for each station, clearly, the best approach would be to use a set of coincident radiosondes and follow the approach described for the Zugspitze in Sect. 2.3 for the other stations. However, if this kind of data is not available for some stations or if the stations have similar geophysical characteristics (IWV levels, station altitude), a simplified approach would be to just use the same value of $\alpha_{opt}=183$ as found for the Zugspitze. However, in so doing one has to take into account that effective regularization strength depends linearly on spectral point spacing p. Therefore, possible station-to-station differences in p should be compensated for by correcting α according to the relation

$$\alpha_{station} \,/\, \alpha_{Zugspitze} = p_{Zugspitze} \,/\, p_{station} \, , \tag{5}$$

with $\alpha_{Zugspitze}=183$ and $p_{Zugspitze}=0.0015\,\mathrm{cm}^{-1}$ as reference.

Finally, harmonizing the procedure for final quality selection of the IWV retrievals at different stations is an important task. For this purpose, a threshold for the root-mean-square (rms) residuals of the spectral fit was used. A value for the threshold was derived by inspection of the probability distribution of all residuals of the Zugspitze time series. This distribution is right skewed with only 5% of the retrievals showing exceptionally high rms residuals. Therefore, the rms threshold was set to exclude these 5%. We found a very similar behavior for the Jungfraujoch retrievals. Therefore, we suggest that to harmonize, a quality selection be made by tuning the threshold for

Full Screen / Esc

Printer-friendly Version

Interactive Discussion

the rms residuals at each station so that ∼5% of the IWV retrievals, i.e. those with the largest residuals, are excluded.

3   Results and discussion

3.1   Harmonized Zugspitze and Jungfraujoch FTIR time series

The Zugspitze (47.4° N, 11.0° E, 2964 m a.s.l) solar FTIR system was set up in 1995 as part of the "Alpine Station" of the NDACC network. It is operated by the Group "Variability and Trends" at IMK-IFU[6], Research Center Karlsruhe, together with a variety of additional sounding systems at the Zugspitze/Garmisch site. These include an NDACC aerosol lidar and an NDACC UV spectroradiometer. The FTIR team contributes to satellite validation and studies of atmospheric variability and trends (e.g., Sussmann and Buchwitz, 2005; Sussmann et al., 2005a, b). The FTIR system is based upon a Bruker IFS125HR interferometer; details can be found in Sussmann and Schäfer (1997). The spectra used for IWV retrieval have been recorded with an optical path difference (OPD) of typically 250 cm, averaging a number of 8 scans (15–20 min integration time). Pressure-temperature profiles, necessary for the inversion, have been taken from the National Center for Environmental Prediction (NCEP) automailer. For quality selection of the IWV retrievals, a threshold for the rms residuals of the spectral fit was used (see Sect. 2.6 for details). The resulting Zugspitze time series including the years 1996–2008 comprises IWV retrievals from a number of 5815 individual spectra as displayed in Fig. 5. The retrievals contain a mean *dofs* of 1.88.

High-resolution FTIR solar absorption spectra are regularly recorded at the Jungfraujoch station (46.5° N, 8.0° E, 3580 m a.s.l.) since 1984, with a home-made instrument installed at the Coudé focus of the Jungfraujoch telescope. In 1990, a commercial

---

[6]Institute for Meteorology and Climate Research – Atmospheric Environmental Research, http://imk-ifu.fzk.de/113.php

Bruker IFS120HR has augmented the observational capacity of the site. Both spectrometers are maintained and operated by the GIRPAS group of the University of Liège (Groupe Infra-Rouge de Physique Atmosphérique et Solaire). More information on these instruments and on important related key findings can be found in Zander et al. (2008) and references therein. Jungfraujoch data are further used for the calibration and validation of atmospheric space-based sensors (e.g., Mahieu et al., 2008). The spectra from the home-made instrument used here have been recorded with OPD of 82 cm, including 7 scans per spectrum for an integration time of 37 min. For the Bruker instrument, the OPD was either equal to 82 or 125 cm, averaging 6 or 18 scans per spectrum, with resulting integration times ranging from 3 to 15 min. Assumed pressure-temperature profiles were also provided by NCEP.

The retrievals of the two different Jungfraujoch FTIRs were harmonized with the optimized, Zugspitze FTIR retrieval as described in Sect. 2.6. In particular, the spectral point spacings of the two Jungfraujoch FTIRs ($0.0061\,\text{cm}^{-1}$ for the home-made instrument and $0.0038\,\text{cm}^{-1}$ for the Bruker) differ from the one of the Zugspitze instrument. Therefore, the regularization strength for each Jungfraujoch FTIR had to be harmonized separately with the Zugspitze instrument according to Eq. (5).

For quality selection of the IWV retrievals, a threshold for the rms residuals was set so as to exclude the highest-rms retrievals (5% of total retrievals) as described above for the Zugspitze. The resulting Jungfraujoch time series from the years 1988–2008 comprises IWV retrievals from a number of 8045 individual spectra as displayed in Fig. 6. The retrievals contain a mean *dofs* of 1.87.

3.2 Trend analysis

The IWV trend results for the Zugspitze and Jungfraujoch time series are given in Table 3. They have been derived according to the approach described in Gardiner et al. (2008). Briefly, the approach augments a basic linear trend model applied to the time series after substraction of a fitted intra-annual function and uses least squares regression in conjunction with a bootstrap resampling of the residuals in order to determine
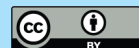
confidence limits associated with the trend estimates. For the inter-annual model, a 3rd order Fourier series (a constant and 3 sine and 3 cosine components) is used. In order to investigate the significance of the trends, the null hypothesis was tested for each analysis to verify that "there is no underlying straight-line trend over the time span of the data", i.e. the gradient of the underlying long-term trend in the regression model is zero. The sampling distribution of the gradient of the underlying straight-line trend term is determined empirically using bootstrap resampling. If the 95% confidence interval associated with the gradient computed from this empirical distribution does not contain zero then, in a formal statistical sense, there is reason to doubt the null hypothesis.

3.3 Discussion of trend results

The trend results given in Table 3 can be summarized as follows:

1. The Zugspitze IWV shows a significant positive trend for all of the analyzed time intervals (1996–2008), (1996–2002), and (2003–2008).

2. The Zugspitze trend in the last 6 years (2003–2008) is significantly higher than in the 7 years before (1996–2002).

3. The Jungfraujoch time series does not show a significant trend for any of the analyzed time intervals (1988–2008), (1996–2008), (1996–2002), or (2003–2008).

We would like to discuss two possible explanations for the significantly different trends above the Zugspitze and Jungfraujoch where either one or both contribute to the observed difference to a certain degree. One interpretation could be that the difference in the altitudes of the Zugspitze (2.96 km a.s.l.) and the Jungfraujoch (3.58 km a.s.l.) is the cause of the observed trend difference. If this were the dominant reason it would mean that the positive Zugspitze trend in IWV originates from a positive trend below 3.58 km altitude. There is some evidence for this hypothesis from the weakly significant positive trend (0.6±0.5 mm/decade) from radiosonde measurements at Payerne (1995–2004), because it is a low altitude site not too far away from the Jungfrau-

Title Page

Abstract | Introduction

Conclusions | References

Tables | Figures

◀ | ▶

◀ | ▶

Back | Close

Full Screen / Esc

Printer-friendly Version

Interactive Discussion

joch. The Payerne trend is confirmed by the TROWARA microwave measurements (0.6 ± 1.5 mm/decade) at Bern (Morland et al., 2006). Together with the finding by Ross and Elliot (2001) that there were no significant lower-tropospheric trends over Europe in the period (1973–1995) this would indicate that the amount of lower tropospheric water vapor has increased after 1995 over Europe.

Another interpretation of the trend difference between the Jungfraujoch and Zugspitze would be that trend measurements of IWV at a certain site are only representative on the regional scale and IWV trends can be significantly different on relatively small spatial scales such as the distance of ~250 km between the Jungfraujoch and the Zugspitze. This interpretation is confirmed by analysis of satellite data which show that globabally in decadal IWV trends, even on this small spatial scale, significant changes of sign of the trends are the rule rather than the exception above land where the correlation to near-surface temperature is less distinct than above the oceans (Vonder Haar et al., 2005; Wanger et al., 2006; Mieruch et al., 2008).

Finally, we want to put our (differing) Zugspitze and Jungfraujoch trend results into a Eurasian to global context which confirms the complexity of the trend picture over the past decades. The main region where positive trends were not evident in the earlier analysis of Ross and Elliott (2001) using data for 1973 through 1995 was over Eurasia and this also appears to be the case from 1988 to 2001 based on ERA-40 data in spite of large, positive trends over the North Atlantic in both SSM/I and ERA-40 data. This is also in spite of generally increasing trends in precipitation in Europe and other mid-latitude regions (Trenberth et al., 2005). However, Philipona et al. (2004) inferred rapid increases in surface water vapor over central Europe during the period from 1995 to 2003. Subsequent analyses (Philipona et al., 2005) confirmed that changes in IWV for this region are strongly coupled to the surface temperature. For central Europe, Auer et al. (2007) demonstrated increasing moisture trends. Mieruch et al. (2008) found increasing IWV trends since 1996 for Greenland, East Europe, Siberia, and Oceania. The large, positive trends from 1973 to 1995 over the USA in IWV appear to have slowed down thereafter and even reversed in the south (Trenberth et al., 2005) and

in the north-west (Mieruch et al., 2008). However, the IWV increase is continuing along the West Coast (in ERA-40 and NCEP) and has picked up in much of Canada (Trenberth et al., 2005). More intense rains have been observed in the USA (Groisman et al., 2004).

4 Conclusions

We have set up a new optimized retrieval of IWV from ground-based, mid-infrared solar FTIR spectrometry based upon a Tikhonov approach constraining the derivative (with respect to height) of the retrieved water profiles given in units of per cent differences relative to an a priori profile. With this method it has been possible to demonstrate, for the first time, a correlation of FTIR retrieved IWV with respect to radiosondes with an ideal slope of 1.00(3); such correlations are the result of an iterative retrieval matching procedure. All other correlation parameters (intercept =0.02(12) mm, bias =0.02(5) mm, $stdv$=0.27 mm, R=0.99) of our FTIR-sonde intercomparison were found to be comparable to or better than example results reported in the literature for sonde intercomparisons of the best among other ground-based IWV sounding techniques (microwave, Raman lidar).

A FTIR-FTIR side-by-side intercomparison reveals a strong exponential increase in the $stdv$ of the coincident IWV differences as a function of increasing temporal mismatch starting at $\Delta t \sim 1$ min. From this we learn that it is difficult, if not impossible, to derive the IWV precision of a ground-based remote sounder from a sonde intercomparison exercise even if the sondes are launched in the close vicinity of the ground-based instrument. This is because it is impossible to reduce Δt below the > 20–30 min ascent time required to reasonably sample the total humidity column by sondes and there is already a significant impact of natural water vapor variability on this time scale. A best estimate for IWV precision is therefore derived from a side-by-side intercomparison of two instruments of the same class because Δt can be reduced down to minutes. We did this with an FTIR-FTIR intercomparison at the Jungfraujoch, where we were able

Trends in integrated water vapor from ground-based FTIR

R. Sussmann et al.

Full Screen / Esc

Printer-friendly Version

Interactive Discussion

Trends in integrated water vapor from ground-based FTIR

R. Sussmann et al.

to derive an upper limit for the precision of 0.05 mm (or 2.2% of the mean IWV). The bias found for the two FTIR instruments used in the side-by-side intercomparison is nearly negligible (0.02(1) mm). Finally, we have presented a harmonization concept so that the new and optimized FTIR retrieval can be implemented at other stations of the

5   NDACC network.

The new IWV retrieval and inter-station harmonization concept was applied to a trend analysis of the two FTIR long term records of the Zugspitze and Jungfraujoch NDACC stations covering the time intervals (1996–2008) and (1988–2008), respectively. The trend analysis comprised an inter-annual model and bootstrap resampling

10   to derive trend significance. For the Zugspitze a significant trend of 0.79 mm/decade was found for the full time period (1996–2008) with an uncertainty interval of (0.65, 0.92) mm/decade (95% confidence). There was a significantly increased trend of 1.41 (1.14, 1.69) mm/decade in the second part of the time series (2003–2008) compared to 0.63 (0.20, 1.06) mm/decade in the first part (1996–2002). For the Jungfraujoch no

15   significant trend was found in any of the investigated periods, i.e. (1988–2008), (1996–2008), (1996–2002), or (2003–2008). It is suggested that the reason why a trend was found at the Zugspitze and not at the Jungfraujoch may be due to the horizontal distance (∼250 km) and/or the altitude difference (3.58–2.96 km) of the two stations. This would imply either an altitude dependency with a significantly higher (positive) trend

20   below 3.58 km than above and/or rather strong regional variations of IWV trends on the scale of 250 km. Our finding is in line with a widespread, complex trend picture over Eurasia during the last decades.

In conclusion we have developed and demonstrated a concept which makes it possible to utilize the existing and ongoing long-term FTIR records of the Zugspitze and

25   Jungfraujoch NDACC stations for IWV trend studies. It has been shown that IWV can be retrieved at two different FTIR stations in a harmonized way and correlated with radiosondes with a slope of 1.00. There are more than a dozen additional solar FTIR records covering more than a decade at stations around the globe operated by NDACC affiliated groups. Therefore, the concepts of our paper provide a basis for upcoming

joint IWV trend studies by the FTIR network. These trend studies will complement existing trend data sets on a global scale which up to now have been based primarily on radiosondes.

References

Auer, I., Böhm, R., Jurkovic, A., Lipa, W., Orlik, A., Potzmann, R., Schöner, W., Ungersböck, M., Matulla, C., Briffa, K., Jones, P., Efthymiadis, D., Brunetti, M., Nanni, T., Maugeri, M., Mercalli, L., Mestre, O., Moisselin, J.-M., Begert, M., Müller-Westermeier, G., Kveton, V., Bochnicek, O., Stastny, P., Lapin, M., Szalai, S., Szentimrey, T., Cegnar, T., Dolinar, M., Gajic-Capka, M., Zaninovic, K., Majstorovic, Z., Nieplova, E.: HISTALP – historical instrumental climatological surface time series of the Greater Alpine Region, Int. J. Climatol., 27, 17–46, 2007.

Christy, J. R., Spencer, R. W., and Lobl, E. S.: Analysis of the merging procedure for the MSU daily temperature time series, J. Climate, 11, 2016–2041, 1998.

Elliott, W. P., Ross, R. J., and Blackmore, W. H.: Recent changes in NWS upper-air observations with emphasis on changes from VIZ to Vaisala radiosondes, B. Am. Meteorol. Soc., 83, 1003–1017, 2002.

Fiorucci, I., Muscari, G., Bianchi, C., Di Girolamo, P., Esposito, F., Grieco, G., Summa, D., Bianchini, G., Palchetti, L., Cacciani, M., Di Iorio, T., Pavese, G., Cimini, D., and de Zafa, R. L.: Measurements of low amounts of precipitable water vapor by millimeter wave spectroscopy: an intercomparison with radiosonde, Raman lidar, and Fourier transform infrared data, J. Geophys. Res., 113, D14314, doi:10.1029/2008JD009831, 2008.

Trends in integrated water vapor from ground-based FTIR

R. Sussmann et al.

Title Page

Abstract	Introduction
Conclusions	References
Tables	Figures

|◄| ►|

◄ | ►

Back | Close

Full Screen / Esc

Printer-friendly Version

Interactive Discussion

Gardiner, T., Forbes, A., de Mazière, M., Vigouroux, C., Mahieu, E., Demoulin, P., Velazco, V., Notholt, J., Blumenstock, T., Hase, F., Kramer, I., Sussmann, R., Stremme, W., Mellqvist, J., Strandberg, A., Ellingsen, K., and Gauss, M.: Trend analysis of greenhouse gases over Europe measured by a network of ground-based remote FTIR instruments, Atmos. Chem. Phys., 8, 6719–6727, 2008,
http://www.atmos-chem-phys.net/8/6719/2008/.

Groisman, P. Y., Knight, R. W., Karl, T. R., Easterling, D. R., Sun, B. M., and Lawrimore, J. H.: Contemporary changes of the hydrological cycle over the contiguous United States: trends derived from in situ observations, J. Hydrometeorol., 5, 64–85, 2004.

Hurrell, J. W. and Trenberth, K. E.: Spurious trends in satellite MSU temperatures from merging different satellite records, Nature, 386, 164–167, 1997.

Hurrell, J. W. and Trenberth, K. E.: Difficulties in obtaining reliable temperature trends: reconciling the surface and satellite microwave sounding unit records, J. Climate, 11, 945–967, 1998.

Leiterer, U., Althausen, D., Franke, K., Katz, A., and Wegner, F.: Correction method for RS80-A Humicap humidity profiles and their validation by lidar backscattering profiles in tropical cirrus clouds, J. Atmos. Ocean. Tech., 22, 18–29, 2005.

Mahieu, E., Duchatelet, P., Demoulin, P., Walker, K. A., Dupuy, E., Froidevaux, L., Randall, C., Catoire, V., Strong, K., Boone, C. D., Bernath, P. F., Blavier, J.-F., Blumenstock, T., Coffey, M., De Mazière, M., Griffith, D., Hannigan, J., Hase, F., Jones, N., Jucks, K. W., Kagawa, A., Kasai, Y., Mebarki, Y., Mikuteit, S., Nassar, R., Notholt, J., Rinsland, C. P., Robert, C., Schrems, O., Senten, C., Smale, D., Taylor, J., Tétard, C., Toon, G. C., Warneke, T., Wood, S. W., Zander, R., and Servais, C.: Validation of ACE-FTS v2.2 measurements of HCl, HF, CCl_3F and CCl_2F_2 using space-, balloon- and ground-based instrument observations, Atmos. Chem. Phys., 8, 6199–6221, 2008,
http://www.atmos-chem-phys.net/8/6199/2008/.

Mieruch, S., Noël, S., Bovensmann, H., and Burrows, J. P.: Analysis of global water vapour trends from satellite measurements in the visible spectral range, Atmos. Chem. Phys., 8, 491–504, 2008,
http://www.atmos-chem-phys.net/8/491/2008/.

Miloshevich, L. M., Vömel, H., Paukkunen, A., Heymsfield, A. J., and Oltmans, S. J.: Characterization and correction of relative humidity measurements from Vaisala RS80-A radiosondes at cold temperatures, J. Atmos. Ocean. Tech., 18, 135–156, 2001.

Title Page

Abstract | Introduction

Conclusions | References

Tables | Figures

◀ | ▶

◀ | ▶

Back | Close

Full Screen / Esc

Printer-friendly Version

Interactive Discussion

Miloshevich, L. M., Paukkunen, A., Vömel, H., and Oltmans, S. J.: Development and validation of a time lag correction for Vaisala radiosonde humidity measurements, J. Atmos. Ocean. Tech., 21, 1305–1327, 2004.

Miloshevich, L. M., Vömel, H., Whiteman, D. N., Lesht, B. M., Schmidlin, F. J., and Russo, F.: Absolute accuracy of water vapour measurements from six operational radiosonde types launched during AWEX-G and implications for AIRS validation, J. Geophys. Res., 111, D09S10, doi:10.1029/2005JD006083, 2006.

Morland, J., Deuber, B., Feist, D. G., Martin, L., Nyeki, S., Kämpfer, N., Mätzler, C., Jeannet, P., and Vuilleumier, L.: The STARTWAVE atmospheric water database, Atmos. Chem. Phys., 6, 2039–2056, 2006,
http://www.atmos-chem-phys.net/6/2039/2006/.

Palm, M., Melsheimer, C., Noël, S., Notholt, J., Burrows, J., and Schrems, O.: Integrated water vapor above Ny lesund, Spitsbergen: a multisensor intercomparison, Atmos. Chem. Phys. Discuss., 8, 21171–21199, 2008,
http://www.atmos-chem-phys-discuss.net/8/21171/2008/.

Philipona, R., Dürr, B., Marty, C., Ohmura, A., and Wild, M.: Radiative forcing – measured at Earth's surface – corroborate the increasing greenhouse effect, Geophys. Res. Lett., 31, L03202, doi:10.1029/2003GL018765, 2004.

Philipona, R., Dürr, B., Ohmura, A., and Ruckstuhl, C.: Anthropogenic greenhouse forcing and strong water vapor feedback increase temperature in Europe, Geophys. Res. Lett., 32, L19809, doi:10.1029/2005GL023624, 2005.

Pougatchev, N. S., Connor, B. J., and Rinsland, C. P.: Infrared measurements of the ozone vertical distribution above Kitt Peak, J. Geophys. Res., 100, 16689–16697, 1995.

Rinsland, C. P., Boughner, R. E., Larsen, J. C., Stokes, G. M., and Brault, J. W.: Diurnal variations of atmospheric nitric oxide: ground-based infrared spectroscopic measurements and their interpretation with time dependent photochemical model calculations, J. Geophys. Res., 89, 9613–9622, 1984.

Randel, D. L., Vonder Haar, T. H., Ringerud, M. A., Stephens, G. L., Greenwald, T. J., and Combs, C. L.: A new global water vapor dataset, B. Am. Meteorl. Soc., 77, 1233–1246, 1996.

Ross, R. J. and Elliott, W. P.: Radiosonde-based Northern Hemisphere tropospheric water vapor trends, J. Climate, 14, 1602–1612, 2001.

Rothmann, L. S., Barbe, A., Benner, D. C., Brown, L. R., Camy-Peyret, C., Carleer, M. R.,

Trends in integrated water vapor from ground-based FTIR

R. Sussmann et al.

Title Page

Abstract	Introduction
Conclusions	References
Tables	Figures

|◄ | ►|

◄ | ►

Back | Close

Full Screen / Esc

Printer-friendly Version

Interactive Discussion

Chance, K., Clerbaux, C., Dana, V., Devi, V. M., Fayt, A., Flaud, J. M., Gamache, R. R., Goldman, A., Jacquemart, D., Jucks, K. W., Lafferty, W. J., Mandin, J. Y., Massie, S. T., Nemtchinov, V., Newnham, D. A., Perrin, A., Rinsland, C. P., Schroeder, J., Smith, K. M., Smith, M. A. H., Tang, K., Toth, R. A., Vander Auwera, J., Varanasi, P., and Yoshino, K.: The HITRAN molecular spectroscopic database: edition of 2000 including updates through 2001, J. Quant. Spectrosc. Ra., 82, 5–44, 2003.

Schneider, M., Hase, F., and Blumenstock, T.: Water vapour profiles by ground-based FTIR spectroscopy: study for an optimised retrieval and its validation, Atmos. Chem. Phys., 6, 811–830, 2006,
http://www.atmos-chem-phys.net/6/811/2006/.

Suortti, T. M., Kats, A., Kivi, R., Kämpfer, N., Leiterer, U., Miloshevich, M. L., Neuber, R., Paukkunen, A., Ruppert, P., Vömel, H., and Yushkov, V.: Tropospheric comparisons of Vaisala radiosondes and balloon-borne frost-point and Lyman-α hygrometers during the LAUTLOS-WAVVAP experiment, J. Atmos. Ocean. Tech., 25, 149–166, 2008.

Sussmann, R. and Schäfer, K: Infrared spectroscopy of tropospheric trace gases: combined analysis of horizontal and vertical column abundances, Appl. Opt., 36, 735–741, 1997.

Sussmann, R. and Camy-Peyret, C.: Ground-Truthing Center Zugspitze, Germany for AIRS/IASI validation, phase I report, EUMETSAT, 18 pp., http://www.imk-ifu.kit.edu/downloads/AIRSVAL_Phase_I_Report.pdf, 2002.

Sussmann, R. and Camy-Peyret, C.: Ground-Truthing Center Zugspitze, Germany for AIRS/IASI validation, phase II report, EUMETSAT, 15 pp, http://www.imk-ifu.kit.edu/downloads/AIRSVAL_Phase_II_Report.pdf, 2003.

Sussmann, R. and Buchwitz, M.: Initial validation of ENVISAT/SCIAMACHY columnar CO by FTIR profile retrievals at the Ground-Truthing Station Zugspitze, Atmos. Chem. Phys., 5, 1497–1503, 2005,
http://www.atmos-chem-phys.net/5/1497/2005/.

Sussmann, R., Stremme, W., Buchwitz, M., and de Beek, R.: Validation of EN-VISAT/SCIAMACHY columnar methane by solar FTIR spectrometry at the Ground-Truthing Station Zugspitze, Atmos. Chem. Phys., 5, 2419–2429, 2005,
http://www.atmos-chem-phys.net/5/2419/2005/.

Sussmann, R., Stremme, W., Burrows, J. P., Richter, A., Seiler, W., and Rettinger, M.: Stratospheric and tropospheric NO_2 variability on the diurnal and annual scale: a combined retrieval from ENVISAT/SCIAMACHY and solar FTIR at the Permanent Ground-Truthing Facil-

ity Zugspitze/Garmisch, Atmos. Chem. Phys., 5, 2657–2677, 2005, http://www.atmos-chem-phys.net/5/2657/2005/.

Sussmann, R. and Borsdorff, T.: Technical Note: Interference errors in infrared remote sounding of the atmosphere, Atmos. Chem. Phys., 7, 3537–3557, 2007, http://www.atmos-chem-phys.net/7/3537/2007/.

Tikhonov, A.: On the solution of incorrectly stated problems and a method of regularization, Dokl. Acad. Nauk SSSR, 151, 501–504, 1963.

Tobin, D. C., Revercomb, H. E., Knuteson, R. O., Lesht, B. M, Strow, L. L., Hannon, S. E.: Feltz, W. F., Moy, L. A., Fetzer, E. J., and Cress, T. S.: Atmospheric radiation measurement site atmospheric state best estimates for atmospheric infrared sounder temperature and water vapor retrieval validation, J. Geophys. Res., 111, D09S14, doi:10.1029/2005JD006103, 2006.

Trenberth, K. E., Fasullo, J., and Smith, L.: Trends and variability in column-integrated atmospheric water vapor, Clim. Dynam., 24, 741–758, doi:10.1007/s00382-005-0017-4, 2005.

Trenberth, K. E., Jones, P. D., Ambenje, P., Bojariu, R., Easterling, D., Klein Tank, A., Parker, D., Rahimzadeh, F., Renwick, J. A., Rusticucci, M., Soden, B., and Zhai, P.: Observations: surface and atmospheric climate change, in: Climate Change 2007: The Physical Science Basis. Contribution of Working Group I to the Fourth Assessment Report of the Intergovernmental Panel on Climate Change, edited by: Solomon, S., Qin, D., Manning, M., et al., Cambridge University Press, Cambridge, UK and New York, NY, USA, 2007.

Vonder Haar, T. H., Forsythe, J. M., McKague, D., Randel, D. L., Ruston. B. C., and Woo, S.: Continuation of the NVAP global water vapor data sets for Pathfinder science analysis, Science and Technology Corporation Technical Report 3333, 44 pp, http://eosweb.larc.nasa.gov/PRODOCS/nvap/sci_tech_report_3333.pdf, 2003.

Vonder Haar, T. H., Forsythe, J. M., Juo, J., Randel, D. L., and Woo, S.: Water vapor trends and variability from the global NVAP dataset, 16th Symposium on Global Change and Climate Variations, 9–13 January 2005, San Diego, California, American Meteorological Society, P5.16, 2005.

Wagner, T., Beirle, S., Grzegorski, M., and Platt, U.: Global trends (1996–2003) of total column precipitable water observed by Global Ozone Monitoring Experiment (GOME) on ERS-2 and their relation to near-surface temperature, J. Geophys. Res., 111, D12102, doi:10.1029/2005JD006523, 2006.

Wang, J., Cole, H. L., Carlson, D. J., Miller, E. R., Beierle, K., Paukkunen, A., and Laine, T. K.:

Trends in integrated water vapor from ground-based FTIR

R. Sussmann et al.

Title Page

Abstract	Introduction
Conclusions	References
Tables	Figures

|◄ | ►|

◄ | ►

Back | Close

Full Screen / Esc

Printer-friendly Version

Interactive Discussion

Corrections of humidity measurement errors from the Vaisala RS80 radiosonde – application to TOGA COARE data, J. Atmos. Ocean. Tech., 19, 981–1002, 2002.

Wentz, F. J. and Schabel, M.: Effects of satellite orbital decay on MSU lower tropospheric temperature trends, Nature, 394, 661–664, 1998.

5   Wentz, F. J. and Schabel, M.: Precise climate monitoring using complementary satellite data sets, Nature, 403, 414–416, 2000.

Zander, R., Mahieu, E., Demoulin, P., Duchatelet, P., Roland, G., Servais, C., De Mazière, M., Reimann, S., and Rinsland, C. P.: Our changing atmosphere: evidence based on long-term infrared solar observations at the Jungfraujoch since 1950, Sci. Total Environ., 391, 184–195,

10   2008.

Trends in integrated water vapor from ground-based FTIR

R. Sussmann et al.

Title Page

Abstract   Introduction

Conclusions   References

Tables   Figures

◄◄   ►►

◄   ►

Back   Close

Full Screen / Esc

Printer-friendly Version

Interactive Discussion

Table 1. IWV correlation parameters from a FTIR side-by-side intercomparison and examples for comparisons of all different ground-based remote techniques versus radiosondes: FTIR, microwave (TROWARA, GBMS), GPS, sun photometer (PFR), and Raman lidar (BASIL). Errors are for 1 sigma confidence, N is the number of coincidences.

	Δt (min)	Δx^a (km)	slope	intercept (mm)	bias (mm)	stdv (mm)	stdv (% of mean)	R	N
FTIR-FTIR[b]	3.75	0	1.001(7)	0.02(2)	0.02(1)	0.07	3.1	0.999	32
FTIR-FTIR[b]	30	0	1.008(4)	0.00(1)	0.02(1)	0.11	4.4	0.998	267
FTIR-FTIR[b]	120	0	1.002(5)	0.03(2)	0.04(1)	0.23	8.0	0.998	773
FTIR-sonde[c]	120	8	1.00(3)	0.02(12)	0.02(5)	0.27	7.9	0.99	25
TROWARA-sonde[d]	120	40	0.88	1.36	0.36	2.02	–	–	–
Jungfraujoch GPS-sonde[d]	30	80	1.12	0.39	0.53	1.39		–	–
Jungfraujoch PFR-sonde[d]	30	80	0.76	0.52	0.08	1.01	–	–	–
FTIR-sonde[e]	120	0	0.85(1)	0.66(9)	–	–	–	–	136
BASIL-sonde[f]	20	0	1.07(2)	−0.04(3)	0.09(2)	0.07	3.6	0.99	17
GBMS-sonde[f]	20	0	0.98(4)	0.08(7)	0.05(3)	0.15	8.9	0.98	23

[a] Distance between ground-based sounder and radiosonde launch site
[b] This work (individual measurements of 2 Jungfraujoch FTIRs)
[c] This work (2 hr-Zugspitze FTIR versus Tobin radiosondes, see Fig. 3c)
[d] Taken from Figs. 9 and 10 in Morland et al. (2006)
[e] Taken from Palm et al. (2008), retrieval different than that in our work
[f] Computed from digitalization of data points of Figs. 6 and 7a in Fiorucci et al. (2008)

Table 2. Precision (1 sigma) and bias of optimized FTIR IWV retrievals derived from a side-by-side intercomparison of two FTIR instruments at the Jungfraujoch.

precision (mm)	precision (% of mean IWV)	bias (mm)	bias (% of mean IWV)
0.05	2.2	0.02(1)	0.96(52)

Table 3. Existence and significance of IWV trends derived from harmonized FTIR measurements at the Zugspitze and Jungfraujoch.

	trend (mm/decade)	uncertainty interval (2.5th percentile, 97.5th percentile)[a] (mm/decade)	significant non-zero trend? (95% confidence)
Zugspitze (1996–2008)	**0.79**	**(0.65, 0.92)**	**yes**
Zugspitze (1996–2002)	**0.63**	**(0.20, 1.06)**	**yes**
Zugspitze (2003–2008)	**1.41**	**(1.14, 1.69)**	**yes**
Jungfraujoch (1996–2008)	0.08	(−0.01, 0.17)	no
Jungfraujoch (1996–2002)	−0.04	(−0.27, 0.19)	no
Jungfraujoch (2003–2008)	0.05	(−0.18, 0.28)	no
Jungfraujoch (1988–2008)	0.04	(−0.01, 0.10)	no

[a] Underlying uncertainty distributions constructed via 5000 bootstrap resamplings for each trend.
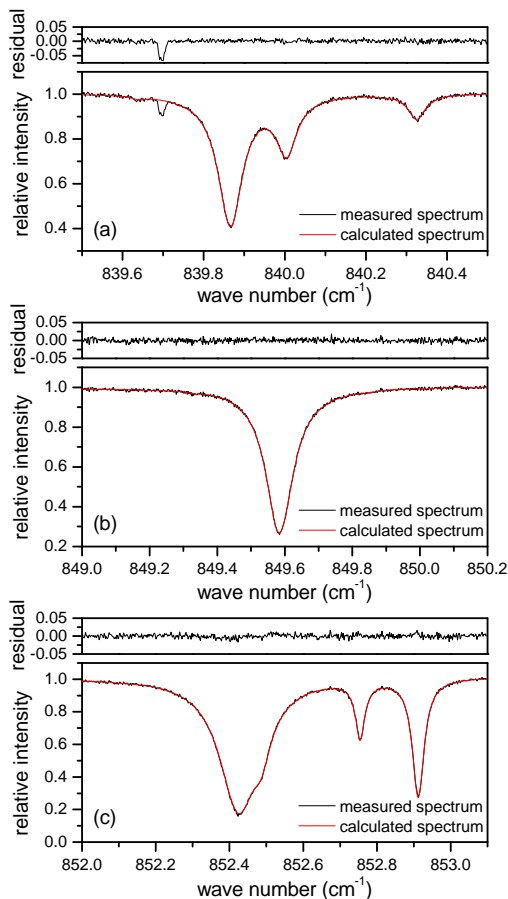
Fig. 1. Spectral intervals **(a–c)** used for FTIR spectrometry optimized for IWV retrieval. The spectrum shown has been recorded with the Zugspitze FTIR at a solar zenith angle of 53.54° and the retrieved IWV is 2.06 mm.
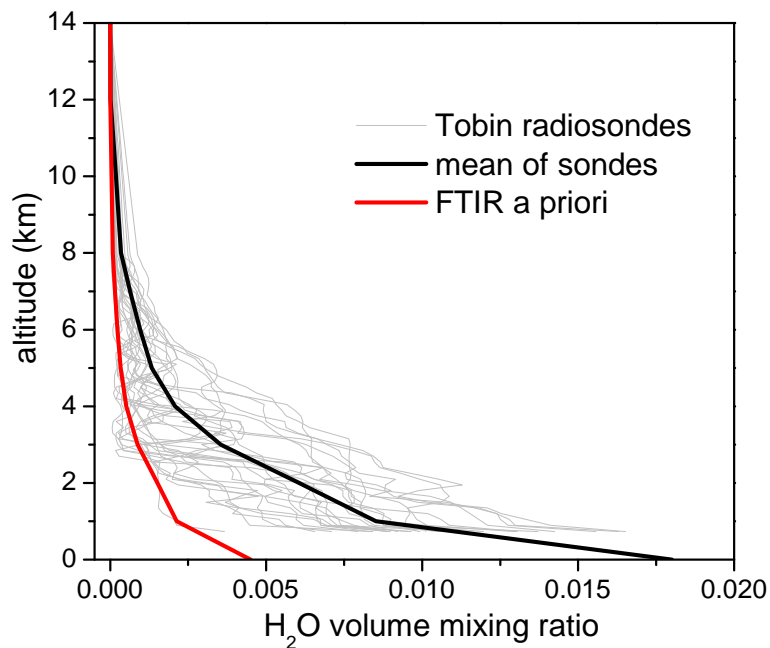
Fig. 2. Garmisch radiosonde data set used for construction of the water vapor a priori profile for the FTIR retrieval of IWV. The 25 "Tobin profiles" shown have been interpolated from 50 individual soundings according to Eq. (4).
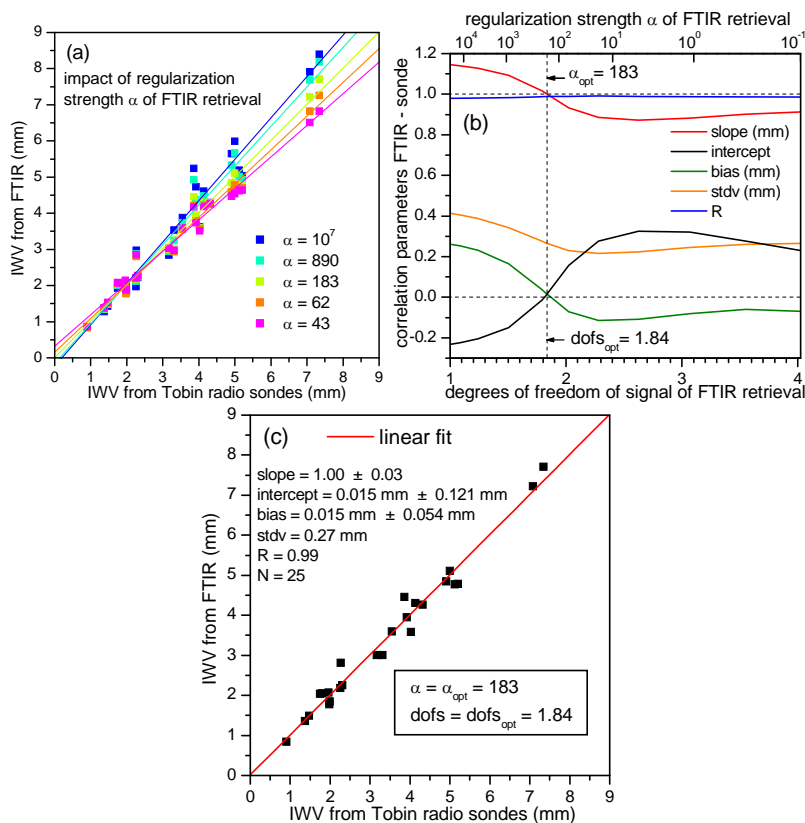
Fig. 3. Procedure for matching FTIR retrievals of IWV to radiosonde characteristics. **(a)** FTIR-sonde scatter plots for different settings of FTIR regularization strength α. **(b)** FTIR-sonde correlation parameters derived from **(a)** as a function of α or dofs(α). **(c)** FTIR-sonde scatter plot for the optimum FTIR retrieval with α_{opt}=183 leading to a slope of 1.00.
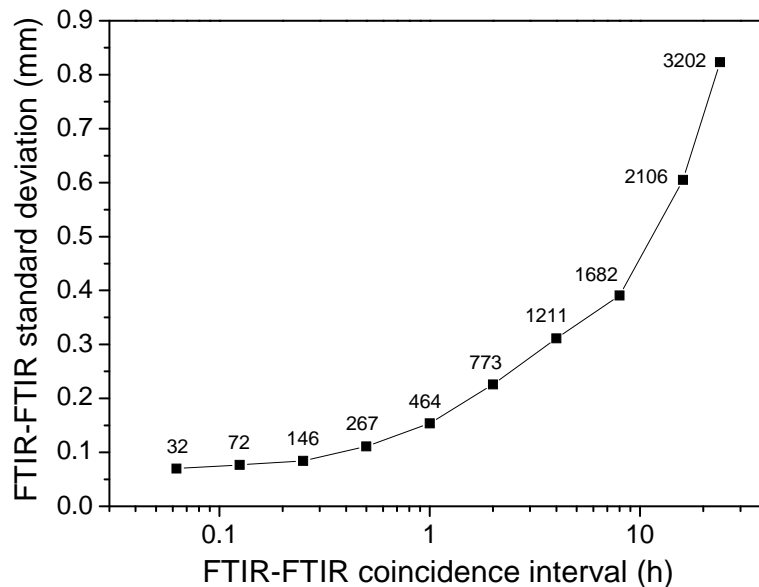
Fig. 4. Standard deviation of the IWV differences deduced from coincident measurements with two FTIR systems at the Jungfraujoch between 1995–2001 as a function of the temporal coincidence criterion (numbers give the amount of coincidences). Note that the exponential increase reflects an atmospheric property (water vapor variability) and is not due to the instruments.
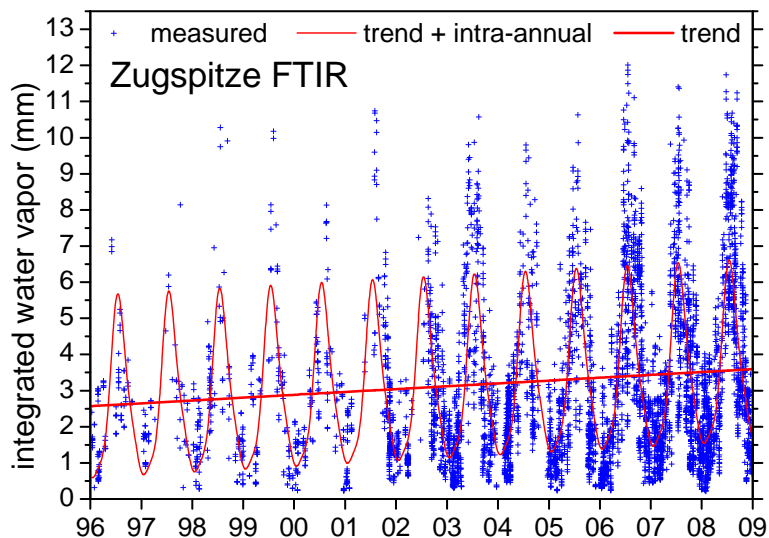
Fig. 5. Time series of Zugspitze (47.4° N, 11.0° E, 2964 m a.s.l) FTIR IWV retrievals from individual measurements (15–20 min integration) matched to radiosonde characteristics. See Table 3 for the trend analysis results.
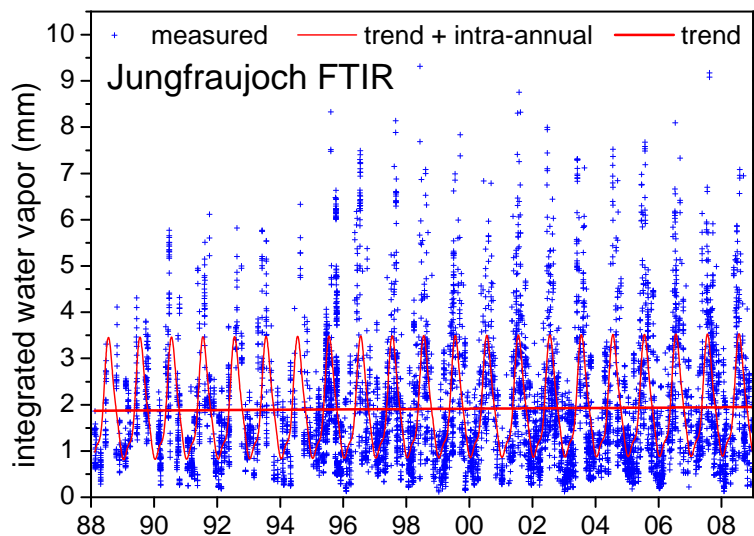
Fig. 6. Time series of Jungfraujoch (46.5° N, 8.0° E, 3580 m a.s.l.) FTIR IWV retrievals from individual measurements (with integration times ranging from 3 to 37 min, depending on the instrument and/or OPD) harmonized with the Zugspitze retrievals. See Table 3 for the trend analysis results.